Acta Mech Sin (2008) 24:223–228
DOI 10.1007/s10409-008-0148-z

TECHNICAL NOTE

Computational fluid dynamics simulations of respiratory airflow in human nasal cavity and its characteristic dimension study

Jun Zhang · Yingxi Liu · Xiuzhen Sun · Shen Yu · Chi Yu

Received: 4 April 2007 / Revised: 26 June 2007 / Accepted: 29 June 2007 / Published online: 15 March 2008
© Springer-Verlag 2008

Abstract To study the airflow distribution in human nasal cavity during respiration and the characteristic parameters of nasal structure, three-dimensional, anatomically accurate representations of 30 adult nasal cavity models were reconstructed based on processed tomography images collected from normal people. The airflow fields in nasal cavities were simulated by fluid dynamics with finite element software ANSYS. The results showed that the difference of human nasal cavity structure led to different airflow distribution in the nasal cavities and variation of the main airstream passing through the common nasal meatus. The nasal resistance in the regions of nasal valve and nasal vestibule accounted for more than half of the overall resistance. The characteristic model of nasal cavity was extracted on the basis of characteristic points and dimensions deduced from the original models. It showed that either the geometric structure or the airflow field of the two kinds of models was similar. The characteristic dimensions were the characteristic parameters of nasal cavity that could properly represent the original model in model studies on nasal cavity.

The project was supported by the National Natural Science Foundation of China (10472025; 10672036) and the Natural Science Foundation of Liaoning Province, China (20032109).
The English text was polished by Yunming Chen.

J. Zhang (✉) · Y. Liu · X. Sun · S. Yu · C. Yu
State Key Laboratory of Structural Analysis for Industrial Equipment, Dalian University of Technology, Dalian 116024, China
e-mail: armyzhang@sina.com

Y. Liu · X. Sun
Department of Otorhinolaryngology, the Second Affiliated Hospital of Dalian Medical University, Dalian 116027, China

Keywords Nasal cavity · Characteristic dimension · Three-dimensional reconstruction · Numerical simulation of flowfield · Computational fluid dynamic · Finite element method

1 Introduction

Nose is the first barrier of defense to outer invasions in the human respiratory system that is protective for life. It performs functions of filtering, warming, and moistening inhaled air and protects the delicate structure of the lower respiratory system. With the development of research on pathogenic mechanism and the application of iatrical apparatus such as endoscopes, it has been demonstrated that certain nasal diseases are closely related to the abnormal structure of nasal cavity [1]. Some researchers have investigated the airflow characters in nasal cavity and tried to find the correlation between the nasal structure and the nasal disease [2], and thus numerical simulations of airflow is surely of considerable help in this field. By simulating the structure and function of the nasal cavity with three-dimensional reconstruction theory with computer, we can explore in detail the outbreak, treatment and prevention of nasal diseases.

Keyhani [3] constructed a finite element mesh of the human nasal cavity from the CAT scans, where the steady-state Navier–Stokes and continuity equations were solved numerically to determine the laminar airflow patterns in the nasal cavity at quiet breathing flow rates, and the numerical results were validated by comparison with detailed experimental measurements of Hahn [4]. Martonen et al. [5] constructed a three-dimensional computational model of human upper-respiratory tract that featured both sides of nasal cavity. The model included airways of the head and the throat based on a cast of a medical school teaching model, and the results

showed airflow patterns corresponding to different flow rates and provided velocity profiles during inhalation and exhalation. Subramaniam et al. [6] presented a three-dimensional, computational model of an adult human's nasal cavity and nasopharynx, and solved the Navier–Stokes and continuity equations for airflow using the finite element method under steady-state inspiratory condition. The model was developed from magnetic resonance imaging scans of a person's nose, and the nasal cavity model was divided into several regions, in which the flow apportionment among different regions of the nose was further detailed. Kim [7] investigated experimentally the airflows in normal and abnormal nasal cavities and surgically created models by particle image velocimetry (PIV), and obtained average distributions of airflow in normal and abnormal nasals. In the case of simulation of surgical operations, the velocity distribution in coronal section was changed locally. Reimersdahl [8] and Hörschler [9] presented numerical simulations of the airflow in a model of human nasal cavity which were found in good agreement with experimental findings. Up to now, few effective principles for describing the nasal cavities with appropriate characteristic parameters of nasal structure have been put forward.

It is essential to build various numerical models to investigate airflow characteristics in different nasal structure which can take difference of individual human nasal cavity into consideration. In this paper, 30 finite element models of nasal cavity of healthy volunteers were reconstructed, and the simulation results gave the distribution of airflow and revealed the relationship between the airflow distribution and the nasal cavity structure. One of these models was compared with its characteristic model in respect of geometrical structure and airflow field to evaluate the feasibility of the method used for extracting characteristic dimensions of human nasal cavities.

2 Methods

2.1 Reconstruction of models

Thirty volunteers (18 males and 12 females aging from 25 to 55 with median 30, Han nationality) were randomly selected from Northeast China. They did not have histories of nasal diseases or any other abnormity in the nasal passages, and were fully examined by nasal anterior rhinoscopy and endoscopy which allowed researchers to qualitatively designate his or her septum as having no deviation. The nasal models were developed from CT scans operated in the Second Affiliated Hospital of Dalian Medical University. The coronal images of nasal cavity at intervals of 3 mm were used to complete the reconstruction since the coronal view could best illustrate nasal structure. With the assistance of a radiologist and a surgeon expertised at nasal CT scans and anatomy, the interface between the nasal mucosa and air in the nasal cavity was delineated from each coronal image which would be linked together to form a three-dimensional model. The models were constructed and meshed automatically by the finite element software of ANSYS after necessary artifact correction was carried out.

The horizontal, sagittal and top views of a meshed nasal model example are shown in Fig. 1. The models at the air outlet were lengthened artificially so that the airflow could fully develop there.

2.2 Numerical simulation

Air is simplified as incompressible fluid. The governing equations for the airflow through the upper airway are the conservation of mass (continuity) and the Navier–Stokes equations, expressed as

$$\begin{aligned}
&\frac{\partial u_x}{\partial x}+\frac{\partial u_y}{\partial y}+\frac{\partial u_z}{\partial z}=0,\\
&\frac{\partial u_x}{\partial t}+u_x\frac{\partial u_x}{\partial x}+u_y\frac{\partial u_x}{\partial y}+u_z\frac{\partial u_x}{\partial z}=-\frac{1}{\rho}\frac{\partial p}{\partial x}+f_x+\upsilon\nabla^2 u_x,\\
&\frac{\partial u_y}{\partial t}+u_x\frac{\partial u_y}{\partial x}+u_y\frac{\partial u_y}{\partial y}+u_z\frac{\partial u_y}{\partial z}=-\frac{1}{\rho}\frac{\partial p}{\partial y}+f_y+\upsilon\nabla^2 u_y,\\
&\frac{\partial u_z}{\partial t}+u_x\frac{\partial u_z}{\partial x}+u_y\frac{\partial u_z}{\partial y}+u_z\frac{\partial u_z}{\partial z}=-\frac{1}{\rho}\frac{\partial p}{\partial z}+f_z+\upsilon\nabla^2 u_z,
\end{aligned}\tag{1}$$

where u_x, u_y, u_z are the velocity components in the Cartesian coordinate and p stands for the pressure. ρ is the mass density of air and υ is its kinematic viscous coefficient.

The nostril (section Ω_1 of Fig. 1) directly opened to the atmosphere with pressure boundary condition $P_{\Omega_1} = 101{,}325\,\text{Pa}$. The interior wall (section Ω of Fig. 1) of the nasal cavity was simplified as a rigid surface since the deformation is slight and consequently little affects the airflow field, and thus the non-slip boundary condition, $u_\Omega = 0$, was assigned to the inner wall. The regular inspiratory capacity for a relaxed, steady inhalation/exhalation is between 400 and 600 ml per period [10] with an inspiratory rate of 15–25 breath/minutes [11] based on medical observations. The upper limit value of 600 ml was adopted in this paper, and it was assumed that the breathing period (the cycle of an inhalation and an exhalation) was 3 s, and airflow velocity varied linearly with time at the exit section as shown in Fig. 2, where the vertical and horizontal axes represented airflow flux and time, respectively. Point a represented the peak value of airflow flux in an inspiration period; point b represented the peak value of airflow flux in an expiration period. At the exit section, the peak velocity was calculated through $u_{\Omega_2} = Q/0.75S$, where Q was the tidal volume and S was the cross sectional area of the exit. The velocity boundary condition could thus be given at the top cross section of the oropharynx (section Ω_2 in Fig. 1) by referring to the above assumptions.

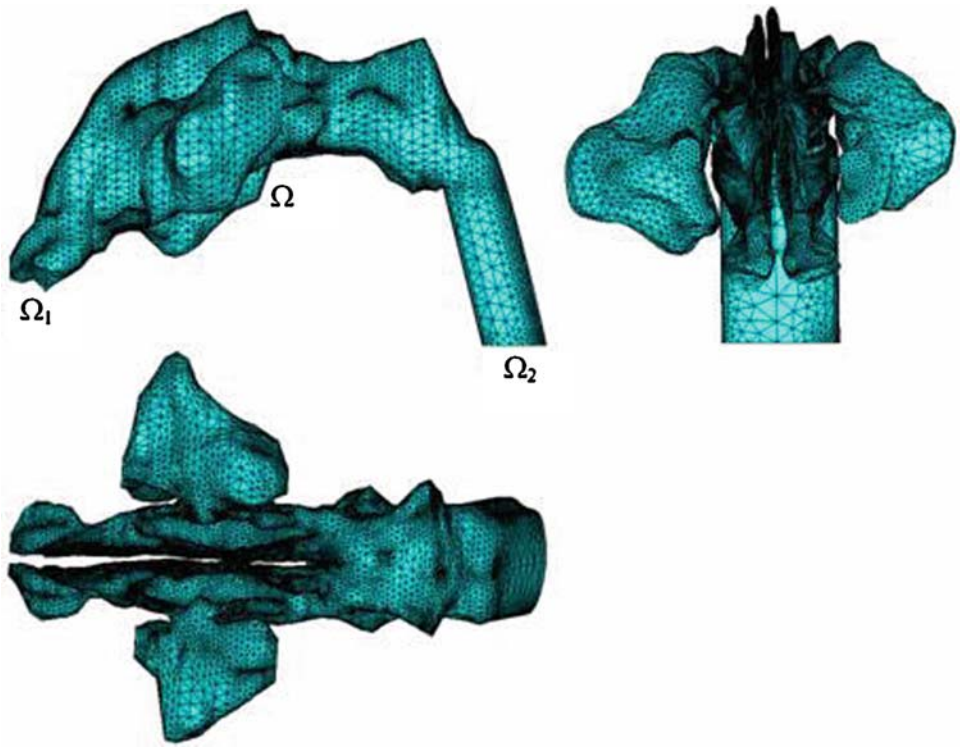

Fig. 1 Three-dimensional reconstruction model of the nasal cavity

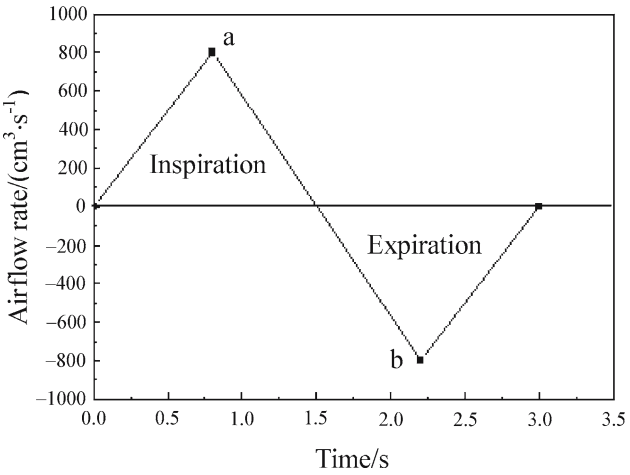

Fig. 2 The change of flow rate with time in a breathing period

Airflow through the nasal cavity was numerically simulated over the entire breathing period after the model was meshed with tetrahedron element. The airflow was described as a transient-state turbulence flow with gas parameters $\rho = 1.25\text{kg/m}^3$, $\upsilon = 1.7894 \times 10^{-5}\text{N s/m}^2$. The standard k–ε turbulent model was adopted in ANSYS.

2.3 Extraction of characteristic dimensions

The nasal cavity was divided into six main parts: nasal vestibule, nasal valve, common nasal meatus, middle nasal meatus, inferior nasal meatus and nasopharynx region, which were defined as characteristic structures of nasal cavity. The proper cross-section of nasal cavity could be found where the middle and inferior turbinates just appeared or disappeared (blue lines in Fig. 3b) and where there was a juncture (red lines in Fig. 3b) of adjacent characteristic structures. These were characteristic sections of the nasal structure where vertexes were defined as characteristic points. The sectional shape of nasal vestibule, nasal valve and nasopharynx were simplified as quadrilaterals, and the width and height were defined as their characteristic dimensions. Anatomy of nasal meatus was much more complex than the others, and thus each meatus was simplified as a corner (as shown in Fig. 3a). Characteristic points in nasal meatus were extracted as shown in Fig. 4 and the widths of nasal meatus were defined as characteristic dimensions. The characteristic nasal cavity model of a volunteer was established in ANSYS based on the coordinate data of the person's characteristic points, and the airflow field was then numerically simulated. The comparison of geometry between the characteristic model and the original one was shown in Fig. 3.

3 Results

3.1 Airflow distribution in the nasal cavity

The pressure and velocity at any point in the nasal cavity could be obtained after numerical simulations for thirty nasal

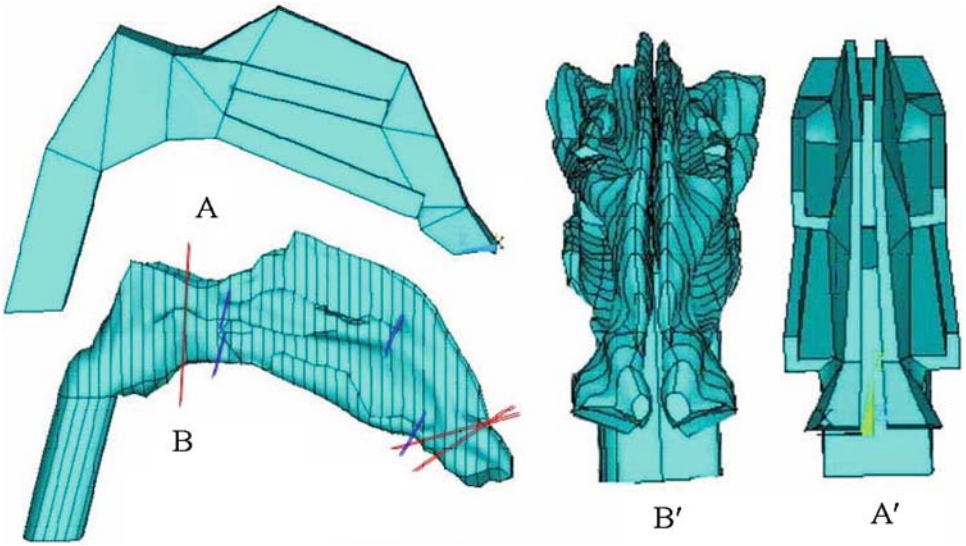

Fig. 3 Comparison between characteristic model and the original one

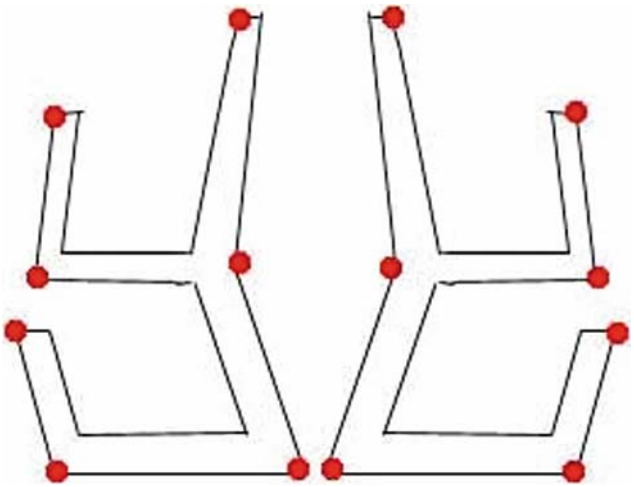

Fig. 4 Extraction of characteristic points in nasal meatus

models were completed. The model shown in Fig. 5 was a replication of a woman's nasal cavity. A slice at a proper position was selected to display the velocity distribution (Fig. 5, left), velocity vectors (Fig. 5, right) and pressure drops (Fig. 5, middle) which presented airflow direction in the nasal cavity at the moment b when the expiratory airflow flux and the pressure drop were at their peak values. The highest airflow velocity appeared in the region of nasal valve. In the region of nasal valve and nasal vestibule, the air pressure changed sharply, but in contrast it changed slowly in the posterior region of nasal proper cavity and the nasopharynx. In these 30 examples, the airflow resistance in the region of 3 cm distance from the nostril accounted for from 50.5% to 77.8% of the overall nasal airway resistances.

Several representative velocity distributions at the moment a were shown in Fig. 6. These figures illustrated that the airflow distribution in each model was a little different and the airflow flux on one side of the nasal cavity was different from that on the other side. The results indicated that there were three airflow distribution modes in the nasal airway:

1. The main stream passed through the common nasal meatus and the residual stream passed through the middle and inferior nasal meatus (shown in Fig. 6, left). In this mode, the airflow flux through the common nasal meatus accounted for 56.6% of the total flux.
2. The main stream passed through the inferior nasal meatus and the common nasal meatus (shown in Fig. 6, middle). In this mode, the airflow flux through inferior nasal meatus and common nasal meatus accounted for 60.5% of the total flux.
3. The main airflow passed through the middle nasal meatus and the common nasal meatus (shown in Fig. 6, right). In this mode, the airflow flux through the middle nasal meatus and the common nasal meatus accounted for 77.0% of the total flux.

Among 30 examples, 7 of them agreed with the first mode; 7 of them were categorized as the second mode. The other 16 examples belonged to the third mode.

By comparing the distribution of velocity field (Fig. 7, left) and the pressure field (Fig. 7, right) between the characteristic model and the original one, it can be concluded that either the geometry structure or the airflow distribution in the characteristic model is similar to those in the original one, and the numerical comparison and the difference are given in Table 1.

4 Discussion

The mechanism of airflow in human nose is important for understanding many aspects of the biology and pathology

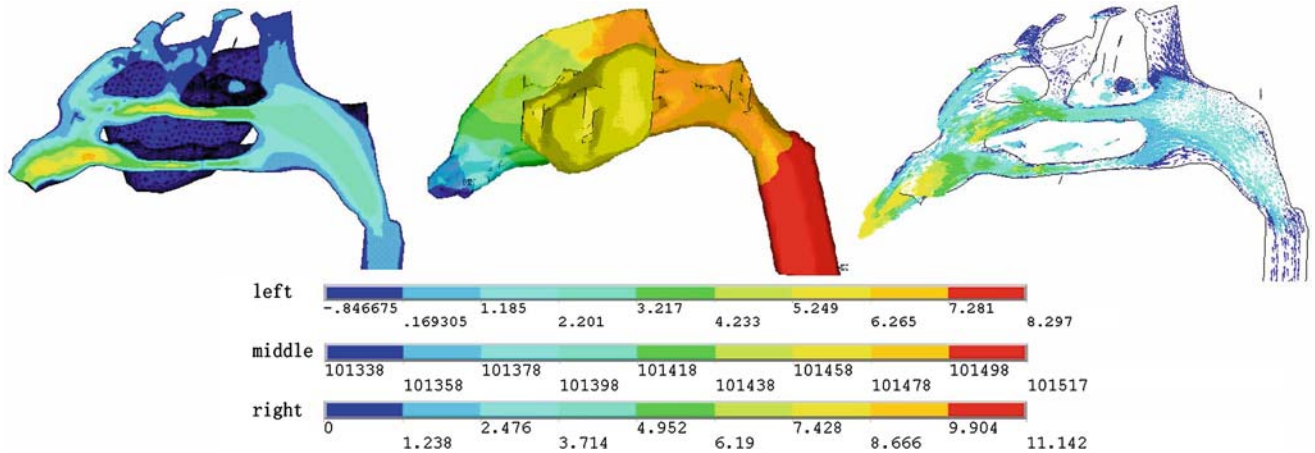

Fig. 5 Velocity (*left*), pressure (*middle*) and vector (*right*) plot at the moment b

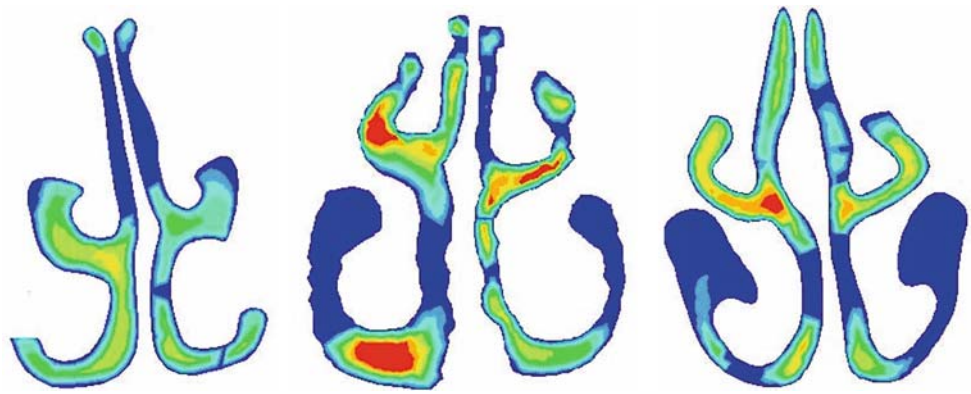

Fig. 6 Distribution of airflow in the nasal passages at the moment of point "a"

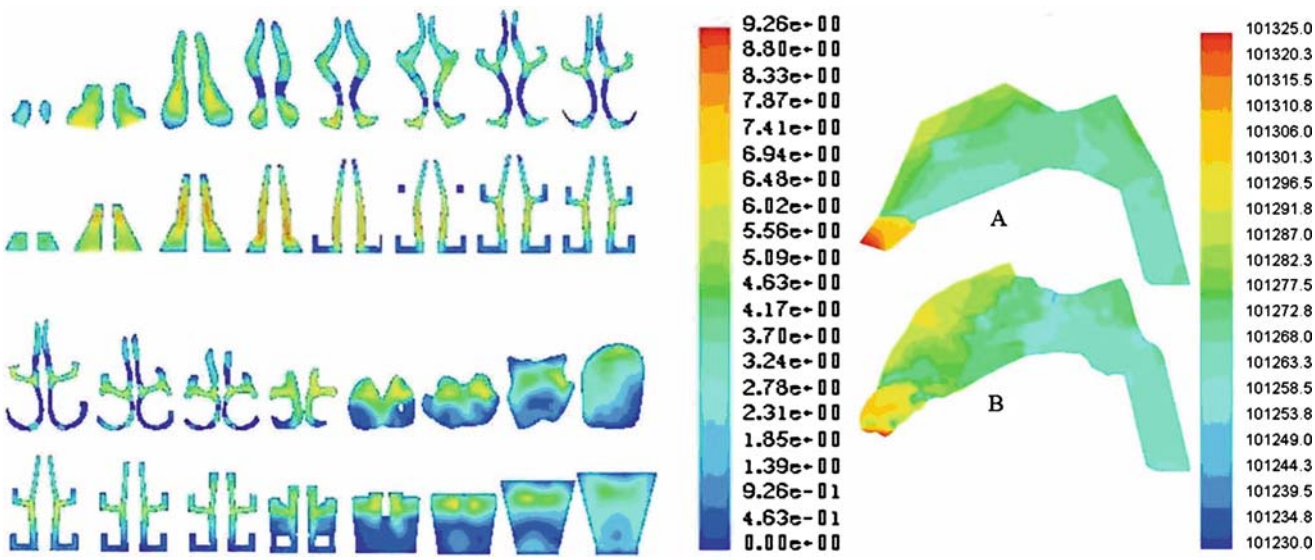

Fig. 7 Comparison of velocity (*left*) and pressure (*right*) distribution between the characteristic model and the origin one of nasal cavity

Table 1 Difference of geometry dimensions and airflow character between two models

	Original model	Characteristic model	Differences/(%)
Cross dimension	0.036 m	0.046 m	12.20
Vertical dimension	0.084 m	0.085 m	0.59
Longitudinal dimension	0.136 m	0.136 m	0.00
Pressure drop	94.8 Pa	79.8 Pa	8.59
Maximal velocity	9.279 m/s	9.260 m/s	0.10

in regard to the respiratory tract. The present investigation showed that the airflow flux through the left or right side of nasal cavity depends on the airflow resistance or the cross-sectional area. On each side, the airflow distribution depends on the structure of airway as the main airflow would pass through the route with wider airway. The resistance is usually lower in the wider airway such as the common nasal meatus or where it intersects with the middle nasal meatus.

Once the representative structural dimensions of nasal cavity is obtained, which were expressed as characteristic points and dimensions in this paper, the airflow distribution in the real nasal cavity could be readily described. The models under the definition of characteristic dimension can represent not only its original model, but also other models with approximately the same characteristic dimensions. Ulyanov [12] provided two typical nasal models classified as the southern type and the northern type. The characters of the northern type nasal cavity were that the inferior turbinate was large in size and the main airflow passed through the middle passage. The characters of southern type nasal cavity were that the inferior turbinate was small in size and the main airflow passed through the inferior interior passage [6]. Because of the large inferior turbinate, the inferior nasal meatus was narrow and the resistance in this airway was high which led to most of airflow passing through the middle nasal meatus. The principle for the southern type nasal cavity was the same as the northern type. This was a good usage of characteristic dimension for identifying humans by his structural character of nasal cavity.

5 Conclusions

A feasible method was developed to reconstruct the numerical models of nasal cavities. Through numerical simulations of thirty examples, the details of airflow distribution in the nasal cavity were illustrated, which showed that the wider the meatus, the more airstream would pass through. The distribution of the airflow would be changed on two sides of the nasal cavity if any part of the nasal structure changed. The numerical model based on characteristic dimension was then reconstructed, which showed that either the geometric structure or the airflow distribution in the characteristic model was similar to those of the original one. And thus conclusion can be drawn that the characteristic model can partly replace the original one and even replace other models with approximately the same characteristic dimensions during model studies on nasal cavity.

Acknowledgments A special note of thanks is extended to radiologist Lai Shengyuan and all the doctors of ENT. Department, Second Affiliated Hospital of Dalian Medical University for their assistance in the design and prosecution of this research.

References

1. Uliyanov, Y.P.: Surgical reconstruction of nasal serodynamics. In: Proceedings of 16th World Congress of Otolaryngol Head and Neck Surg., XVI World Congress of Otolaryngol Head and Neck Surg, Sydney, Australia, pp. 1591–1595 (1997)
2. Liu, Y.X., Yu, S., Sun, X.Z., et al.: Structure of nasal cavity and characters of airflow. Chin. J. Otorhinolaryngol Head Neck Surg. **40**(11), 846–849 (2005)
3. Keyhani, K., Scherer, P.W., Mozell, M.M.: Numerical simulation of airflow in the human nasal cavity. J. Biomech. Eng. **117**, 429–441 (1995)
4. Hahn, I., Scherer, P.W., Mozell, M.M. et al.: Velocity profiles measured for airflow through a large scale model of he human nasal cavity. J. Appl. Physiol. **75**, 2273–2287 (1993)
5. Martonen, T.B., Quan, L., Zhang, Z., et al.: Flow simulation in the human upper respiratory tract. Cell Biochem. Biophys. **37**, 27–36 (2002)
6. Subramaniam, R.P., Richardson, R.B., Morgan, K.T.: Computational fluid dynamics simulations of inspiratory airflow in the human nose and nasopharynx. Inhalation Toxicol. **10**, 91–120 (1998)
7. Kim, S.K., Chung, S.K.: An investigation on airflow in disordered nasal cavity and its corrected models by tomographic PIV. Meas. Sci. Technol. **15**, 1090–1096 (2004)
8. Reimersdahl, Th., Hörschler, I., Gerndt, A.: Airflow simulation inside a model of the human nasal cavity in a virtual reality based rhinological operation planning system. Int. Congr. Serg. **1230**, 87–92 (2001)
9. Hörschler, I., Meinke, M., Schröder, W.: Numerical simulation of the flow field in a model of the nasal cavity. Comput. Fluids **32**, 39–45 (2003)
10. Guitong, Y., Weiyi, C., Jinbin, X.: Biomechanics. Chongqing Press, Chongqing (1999)
11. keyhani, K., Scherer, P.W.: Numerical simulation of airflow in the human nasal cavity. J. Biomech. Eng. **117**, 429–441 (1995)
12. Ulyanov, Y.P.: Clinical manifestations the variants of nasal aerodynamics. Otolaryngol Head Neck Surg. **119**, 152–153 (1998)